Inverse Compton Scattering in Mildly Relativistic Plasma

S. M. Molnar[1,2]
Laboratory for High Energy Astrophysics, Code 662
Goddard Space Flight Center
Greeenbelt, MD 20771

IN-75
410 909

M. Birkinshaw[3]
Department of Physics, University of Bristol,
Tyndall Avenue, Bristol, BS8 1TL, UK

ABSTRACT

We investigated the effect of inverse Compton scattering in mildly relativistic static and moving plasmas with low optical depth using Monte Carlo simulations, and calculated the Sunyaev-Zel'dovich effect in the cosmic background radiation. Our semi-analytic method is based on a separation of photon diffusion in frequency and real space. We use Monte Carlo simulation to derive the intensity and frequency of the scattered photons for a monochromatic incoming radiation. The outgoing spectrum is determined by integrating over the spectrum of the incoming radiation using the intensity to determine the correct weight. This method makes it possible to study the emerging radiation as a function of frequency and direction. As a first application we have studied the effects of finite optical depth and gas infall on the Sunyaev-Zel'dovich effect (not possible with the extended Kompaneets equation) and discuss the parameter range in which the Boltzmann equation and its expansions can be used. For high temperature clusters ($k_B T_e \gtrsim 15$ keV) relativistic corrections based on a fifth order expansion of the extended Kompaneets equation seriously underestimate the Sunyaev-Zel'dovich effect at high frequencies. The contribution from plasma infall is less important for reasonable velocities. We give a convenient analytical expression for the dependence of the cross-over frequency on temperature, optical depth, and gas infall speed. Optical depth effects are often more important than relativistic corrections, and should be taken into account for high-precision work, but are smaller than the typical kinematic effect from cluster radial velocities.

Subject headings: (cosmology:) cosmic microwave background — galaxies: clusters: general — methods: numerical — plasmas — scattering

---

[1]NAS/NRC Research Associate

[2]previous address: Department of Physics, University of Bristol, Tyndall Avenue, Bristol, BS8 1TL, UK

[3]also: Center for Astrophysics, 60 Garden Street, Cambridge, MA 02138, USA

1. Introduction

Inverse Compton scattering of the cosmic microwave background radiation (CMBR) by hot electrons in the atmospheres of clusters of galaxies, the Sunyaev-Zel'dovich (SZ) effect (Sunyaev and Zel'dovich 1980), has become a powerful tool in astrophysics. It is one of the most important secondary effects which cause fluctuations in the CMBR. We will refer to the effect arising from static gas as the static SZ (SSZ) effect, and that arising from gas with bulk motion as the kinematic SZ (KSZ) effect. Fluctuations in the CMBR caused by the SZ effects in an ensemble of clusters of galaxies should dominate on angular scales less than few arcminutes. The nature of these fluctuations depends on the evolution of clusters, and so it is a test of structure formation theories (eg. Aghanim et al. 1998; Molnar and Birkinshaw 1998).

Observations of the SSZ effect, begun in the 1970s, have now become routine in the 90s with dedicated instruments using the latest receiver technology (for reviews see Rephaeli 1995b; Birkinshaw 1998). SZ effect and x-ray measurements probe the physical conditions in the intracluster gas in clusters of galaxies, and allow us to deduce the distance to the cluster without additional assumptions. This provides a useful independent method for determining the Hubble constant.

Observations of the KSZ effect are much more difficult since it is typically an order of magnitude smaller than the SSZ effect and has the same spectrum as the primordial fluctuations in the CMBR. The KSZ effect provides a method of measuring radial peculiar velocities of clusters, and even without the tangential velocity component, which might be determined using the Rees-Sciama (RS) effect (Rees and Sciama 1968; Birkinshaw and Gull 1983; Gurvits and Mitrofanov 1986; Aghanim et al. 1998; Molnar and Birkinshaw 1998) it should provide important information on large scale velocity fields, which are closely related to the large scale density distributions and thus to the average total mass density in the Universe. Useful limits on the size of the KSZ effect for two clusters have recently been reported by Holzapfel et al. (1997a).

Most discussions of the SSZ effect have been based on non-relativistic calculations of its amplitude, made via a Fokker-Planck type expansion of the Boltzmann equation (Kompaneets 1957). The advantage of this approach is that in interesting cases (electron temperature, T_e, much greater than the temperature of the incoming radiation) it provides a convenient analytical solution for the spectrum of the emerging radiation. However, it has been recognized recently that relativistic effects become important for clusters with $kT_e \gtrsim 10$ keV. Rephaeli (1995a) provided a relativistic solution for the SSZ effect as a series expansion in the optical depth ($\ll 1$ for clusters). There is no exact analytical solution. The numerical integrals involved are tractable in the single-scattering approximation, which is usually adequate in clusters. Fargion, Konoplich and Salis (1996) developed exact expressions for relativistic inverse Compton scattering of a laser beam with monochromatic isotropic radiation, finding good agreement with the approximations of Jones (1968). Their expression for the frequency redistribution function (FRDF) for scattering of monoenergetic electrons with monochromatic photons agrees with Rephaeli's result. Rephaeli's

method has been used in a series of papers to evaluate the SSZ effect for hot clusters. Relativistic corrections to the SSZ effect, and to the standard thermal bremsstrahlung formulae, were applied to determine the Hubble constant in hot clusters by Rephaeli and Yankovich (1997), however, their corrections of the thermal bremsstrahlung equation were further corrected by Hughes and Birkinshaw (1998). Holzapfel et al. (1997b) used the relativistic results in their determination of the Hubble constant from observations of cluster Abell 2163.

The most general treatment of Compton scattering in static and moving media has been derived by Psaltis and Lamb (1997) as a series expansion. As Challinor and Lasenby (1998b) noted, however, more terms in the expansion should be taken into account for accurate treatment of clusters of galaxies. Recently the Kompaneets equation has been extended to contain relativistic corrections to the SSZ and KSZ effects (Stebbins 1997; Challinor and Lasenby 1998a, b; Itoh, Kohyama and Nozawa 1998; Nozawa, Itoh and Kohyama 1998; Sazonov and Sunyaev 1998b). Starting from the Boltzmann equation, an expansion in the small parameters of the dimensionless temperature, $\Theta_e = kT_e/(m_e c^2)$, fractional energy change in a scattering, $(h\nu' - h\nu)/k_B T_e$, and dimensionless radial velocity for the KSZ effect, v_{rad}/c, leads to a Fokker-Planck type equation (the extended Kompaneets equation). Corrections up to the fifth order in Θ_e have been derived (Itoh et al. 1998). These calculations demonstrate the importance of the relativistic effects (in accordance with the results of Rephaeli 1995a). Note however, that, as Challinor and Lasenby (1998a) emphasized, the extended Kompaneets equation is a result of an asymptotic series expansion, therefore it is important to estimate the validity of the expansion using other methods. Nozawa et al. compared the convergence of their expansion to a direct numerical evaluation of the Boltzmann collision integral, and concluded that in the Rayleigh-Jeans region the relativistic corrections give accurate results in the entire range of cluster temperatures. Significant deviations are found at higher frequencies for high temperature clusters.

The SSZ and KSZ effects must be separated in order to extract information on peculiar velocities. Fortunately the two effects have different frequency dependence. The maximum of the KSZ effect (in thermodynamic temperature units) occurs at about the "cross-over" frequency where the SSZ effect changes sign from being a decrement to an increment. In a non-relativistic treatment the cross-over frequency is a constant, 218 GHz, independent of electron temperature, optical depth, and all other parameters. Rephaeli (1995a) showed that in the relativistic case the cross-over frequency depends on the temperature, and his results were used by Holzapfel et al. (1997a) in determining peculiar velocities of two clusters. Sazonov and Sunyaev (1998b) and Nozawa et al. (1998) give approximations for the cross-over frequency as a function of dimensionless temperature and radial peculiar velocity. They also conclude that relativistic corrections to the cross-over frequency are important, and should be taken into account in future experiments.

Other methods have been used to investigate inverse Compton scattering, such as numerical integration of the collision integral (Corman 1970), multiple scattering methods (Wright 1979), and Monte Carlo simulations. Simulations of inverse Compton scattering in relativistic and

non-relativistic plasma have been carried out for embedded sources (Pozdnyakov, Sobol, and Sunyaev 1983; Haardt and Maraschi 1993; Hua and Titarchuk 1995). Gull and Garret (1998) used Monte Carlo methods to evaluate the Boltzmann collisional integral. Sazonov and Sunyaev (1998a) used Monte Carlo simulations to derive the SZ thermal and kinematic effects.

In this paper we study the effect of optical depth and non-uniform bulk motion on the SZ effect using a Monte Carlo method to calculate the frequency redistribution function. The inverse Compton scattering of CMBR photons is treated in the Thomson limit for static and infalling plasmas (SSZ and KSZ effects) with spherical symmetry, uniform density distribution, and low optical depth over a wide range of gas temperatures and observed frequency. We apply our results to clusters of galaxies assuming a static and radially infalling (or collapsing) gas component.

2. The Method

2.1. Formalism

The emerging intensity of a beam of radiation in the line of sight after passage through a scattering atmosphere can be expressed as

$$I(x) = e^{-\tau} B(x) + I_{sc}(x), \tag{1}$$

where the incoming intensity (hereafter assumed to be Planckian), $B(x)$, is attenuated by a factor depending on the optical depth τ and we add the scattered intensity into the beam, I_{sc}, at dimensionless frequency $x = h\nu/k_B T_{CB}$, where h, ν, k_B and T_{CB} are the Planck constant, the frequency, the Boltzmann constant, and the temperature of the CMBR, $T_{CB} = 2.728 \pm 0.002$ K (Fixsen et al. 1996). The scattered intensity may be determined by using

$$I_{sc}(\nu) = \int P(s)\, B_{sc}(\nu_0) ds, \tag{2}$$

where the intensity of the scattered incoming radiation $B_{sc}(\nu) = w_{sc} B(\nu)$, and w_{sc} is the fraction of photons scattered into the beam, the weight for this beam. $P(s)$ is the frequency redistribution function (FRDF), which specifies the probability of scattering from ν_0 to ν as a function of the logarithm of the dimensionless frequency $s = \ln(\nu/\nu_0)$. This function gives the frequency distribution (normalized to unity) of the scattered radiation (we give $P(s)$ a slightly different definition from the one given by Birkinshaw 1998). This decomposition is possible because in our approximation the fractional frequency change is independent of the frequency (see equation 16 later). The change of the intensity in the line of sight may be expressed as

$$\Delta I(x) = (e^{-\tau} - 1) B(x) + I_{sc}(x). \tag{3}$$

For isotropic and homogeneous scattering conditions, so that the scattering parameters do not depend on where the scattering happens, the weight

$$w_{sc} = (1 - e^{-\tau}), \tag{4}$$

which means that the out-scattered radiation is balanced by the same amount of in-scattered radiation, and so there would be no net intensity change ($\Delta I(x) = 0$) if there were no frequency change ($P(s)$ is the Dirac delta function). This assumption breaks down, for example, when there is relativistic bulk motion, which introduces anisotropy in the scattering via the relativistic beaming effect. Our task is to determine $P(s)$ and w_{sc}. We used equation (4) as a check for our Monte Carlo simulations for static models (where it must be correct), and verified that it is a good approximation for our models with infall by counting outgoing photons. We derive $P(s)$ using a Monte Carlo method. At low optical depth ($\tau \lesssim 1$), the problem is suitable for Monte Carlo simulation because we do not have to follow photons through many scatterings in the medium (the average number of scatterings being τ). Although in this limit most of the photons do not scatter, and hence provide no information on $P(s)$, this is not a problem since we can use the method of forced first scattering (see below).

2.2. Monte Carlo Method

We give a short description of the method here, for a more detailed description see Molnar (1998).

We assume an isotropic incoming low temperature radiation field (the CMBR). We use forced first scatterings to study the inverse Compton process. The photons Compton scatter from an electron population with a relativistic Maxwellian distribution of momenta in the rest frame of bulk motion. We compute scattering probabilities in the rest frame of the electron in the Thomson limit (Chandrasekhar 1950). This involves coordinate transformations from the observer's frame to the rest frame of the bulk motion and to the rest frame of the electron. We assume time translation invariance and spherical symmetry. Time translational invariance is not exact for our model with infall, so that we make a snap-shot approximation. The error arising from this approximation is less than the light crossing time over the infall time ($\approx v_r/c = \beta_r$), which is only a few per cent of the infall term for our models.

In most cases we use the inverse method to generate the desired probability distribution. We use a rejection method when the inverse method leads to non-invertible functions or is too slow: for a general description of generating probability distributions cf. Pozdnyakov et al. (1983); Press et al. (1992). The former reference describes an alternative Monte Carlo method to treat inverse Compton scattering.

In the description that follows we use the word "photon" in the singular to refer to one Monte

Carlo "photon", one experiment in our simulation. We use a weight, w_{in}, to express the number of photons this one experiment represents (the weight does not have to be an integer). We carried out the simulation in five steps.

Step 1. The position and direction of incoming photons:

We assume that the photons arrive uniformly on a unit sphere (the radius of the gas is scaled to unity). In a coordinate system which is placed at the point of impact, the direction cosine of the incoming photons from the normal, μ_{in}, can be sampled as

$$\mu_{in} = \sqrt{[RN]}, \tag{5}$$

where we use $[RN]$ to indicate a uniformly distributed random number drawn each time when it occurs. The azimuthal angle is assumed to be uniformly distributed between 0 and 2π.

Step 2. distance to the forced first scattering:

We use forced first scattering, which means that we take the probability of scattering equal to one on the photons' original line of flight through the gas. Using the inversion method, the optical depth at which the incoming photon scatters becomes

$$\tau_1 = -\ln(1 - [RN] \cdot (1 - e^{-\tau^0_{max}})), \tag{6}$$

where τ^0_{max} is the maximum optical depth in the line of sight (the superscript refers to the number of times the photon has already scattered; zero in this case). Since we are using forced first collisions, we have to account for the fraction of photons which are unscattered on their path through the cloud. The scattered weight may be obtained from equation (4): $w_{sc} = (1 - e^{-\tau^0_{max}})w_{in}$, and stays the same during subsequent (unforced) scatterings. The weight of the photons passing through the cloud without scattering is $w_{out} = w_{in}e^{-\tau^0_{max}}$.

Step 3. scattering:

At the calculated position of the (forced first) scattering, we use the direction of the incoming photon and obtain the direction of propagation and frequency of the scattered photon. In the case that the gas is moving, we make a Lorentz transformation into the rest frame of the moving plasma. We sample the scattered electron's dimensionless velocity, $\beta_e = v_e/c$, from a relativistic Maxwellian distribution

$$P(\beta_e)\, d\beta_e = N_{rel}\, \beta_e^2\, \gamma^5\, e^{-\gamma/\Theta_e}\, d\beta_e, \tag{7}$$

where the normalization is

$$N_{rel} = \left(\Theta_e\, K_2(1/\Theta_e)\right)^{-1}, \tag{8}$$

K_2 is the second order modified Bessel function of the second kind, and the dimensionless electron temperature is

$$\Theta_e = \frac{k_B T_e}{m_e c^2}. \tag{9}$$

We used the rejection method to sample β_e.

The distribution of the direction of electron momenta is simplest in a frame in which the photon momentum unit vector points into one of the coordinate axes, z for example. In this coordinate system the probability distribution of μ_e, the cosine of the angle between the unit vector of the direction of photon propagation (z axis) and electron velocity, is

$$P(\mu_e, \beta_e) = (1 - \beta_e \mu_e)/2. \tag{10}$$

The inversion method leads to sampling μ_e as

$$\mu_e = \frac{1}{\beta_e}\left(1 - \sqrt{1 - 2\beta_e\left(2[RN] - 1 - \frac{\beta_e}{2}\right)}\right), \tag{11}$$

where the sign of the square root was determined so that in the limit of small electron velocities we recover the result for an isotropic distribution ($\mu_e = 2[RN] - 1$). The angular distribution of the scattered electrons in the plane perpendicular to the momentum vector of the photon is isotropic (at azimuthal angle uniformly distributed between 0 and 2π). In the rest frame of the electron, the cosine of the polar angle of the incoming photon is derived from a Lorentz transformation as

$$\mu = \frac{-\mu_e + \beta_e}{1 - \beta_e \mu_e}, \tag{12}$$

where the negative sign in front of μ_e is appropriate for an *incoming* photon. In the electron's rest frame the scattering probability of a photon coming in with direction cosine μ and leaving with direction cosine μ' is given by Chandrasekhar (1950)

$$f(\mu, \mu') = \frac{3}{8}\left(1 + \mu^2 \mu'^2 + \frac{1}{2}(1 - \mu^2)(1 - \mu'^2)\right). \tag{13}$$

μ' can be sampled using a uniform probability distribution by inversion of

$$[RN] = \int_{-1}^{\mu'} f(\mu, \mu') d\mu = \frac{3}{16}\left((\mu^2 - \frac{1}{3})\mu'^3 + (3 - \mu^2)\mu' - \frac{8}{9}\right), \tag{14}$$

which leads to a cubic equation for μ',

$$\left(\mu^2 - \frac{1}{3}\right)\mu'^3 + \left(3 - \mu^2\right)\mu' - \frac{8}{3}\left(2\,[RN] + \frac{1}{3}\right) = 0. \tag{15}$$

This cubic equation has a single real solution with absolute value of μ' less or equal to one. We now transfer the direction and frequency of the scattered radiation back to the observer's frame. The dimensionless outgoing frequency of the photon normalized to the incoming frequency (expressed with the s parameter) becomes

$$s = \ln \frac{\nu'}{\nu_0} = \ln\Big(\gamma_e^2\big(1 - \beta_e\mu_e\big)\big(1 + \beta_e\mu'\big)\Big). \tag{16}$$

Step 4. loop over scatterings:

Having the point of scattering, the scattered frequency, and the direction of the scattered photon, we now sample the optical depth to the next scattering. We do not use forced scattering, so the optical depth follows from the usual (inverse) method as

$$\tau_n = -\ln[RN], \tag{17}$$

where the lower index on τ refers to the nth scattering ($n > 1$), and we used $[RN] = 1 - [RN]$, which is correct for uniform probability distributions. If τ is less than the maximum optical depth in the direction of the photon momentum after the previous scattering, τ_{max}^{n-1}, the photon is taken to have scattered within the cloud, and we calculate the new scattering direction and frequency of the scattered photon as in step 3. If $\tau_n > \tau_{max}^{n-1}$, the photon escaped (scattered $n-1$ times), and we register the impact parameter (with the weight of the photon) and the dimensionless frequency, s, of the escaped photon. At the end of the simulation we sum the weights in every impact parameter bin to check our assumption of homogeneous scattering (equation 4).

Step 5. The frequency redistribution function:

When the simulation finishes, we derive the FRDF by binning the frequencies of the out-coming photons. The discrete probability distribution then becomes

$$P(s_k) = N_s \mathcal{N}_k. \tag{18}$$

$\mathcal{N}_k$ is the number of photons in the k$^{\text{th}}$ bin, for which $s_k - \Delta s/2 \leq s < s_k + \Delta s/2$, where s_k is the center of the kth bin, Δs is the width of the bin, and N_s is the normalization, $N_s = 1/(\Delta s N_{MC})$. N_{MC} is the number of Monte Carlo photons. This $P(s_k)$ is our sampled approximation to $P(s)$, and we then fit an exponential of polynomials to $P(s_k)$ to get a convenient expression for the FRDF. Our fit gives an approximation accurate to better than half a percent, except in the (small) extended tails, where $P(s)$ is under-represented. However, these regions lie 3 orders of magnitude below the peak, and the error arising from the fit is negligible for our applications.

2.3. Testing the code

2.3.1. Single-scattering approximation

We tested our code by comparing our single scattering Monte Carlo results for the FRDF (P_1^{MC}) to those derived from Rephaeli (1995a). Rephaeli's single-scattering approximation can be written as

$$P_1(s) = \frac{3}{32\,N_{rel}} \int_{\beta_0}^{1} \gamma\, e^{-\gamma/\Theta_e} \beta_e^{-4} (f_1 + f_2 + f_3)\, d\beta_e, \tag{19}$$

where

$$\begin{aligned} f_1 &= e^{3s}\beta_e^3(\mu_2^3 - \mu_2 - \mu_1^3 + \mu_1) \\ f_2 &= \left(\beta_e^2 - 3(4e^s + 1) + 3\,e^s(x_2 + x_1) + \frac{2\beta_e^2 - 3(1+\beta_e^4)}{x_2\,x_1}\right) e^s\,(x_2 - x_1) \\ f_3 &= 2e^s\,(e^s + 1)(3 - \beta_e^2) \ln\frac{x_2}{x_1}, \end{aligned} \tag{20}$$

where $x_1 = 1 - \beta_e\,\mu_1$, $x_2 = 1 - \beta_e\,\mu_2$, μ_1 and μ_2 are defined by

$$\begin{aligned} \mu_1 &= \begin{cases} -1 & s \le 0 \\ \frac{1-e^{-s}(1+\beta_e)}{\beta_e} & s \ge 0 \end{cases} \\ \mu_2 &= \begin{cases} \frac{1-e^{-s}(1-\beta_e)}{\beta_e} & s \le 0 \\ 1 & s \ge 0 \end{cases}, \end{aligned} \tag{21}$$

and we used equation (16) to eliminate μt. This result (equation [19]) agrees with Fargion et al. (1996). These expressions can be integrated numerically, except when $s = 0$. In that case $\beta_0 = 0$, and direct numerical integration is not possible because of the diverging β_e^{-4} term. For small β_e ($\beta_e < b = 0.1$ for example) we can expand the logarithm, and use this expansion as a good approximation. For $s = 0$, equation (19) becomes

$$P_1(s=0) = \frac{3}{8\,N_{rel}} \left(\int_0^b f_0\, d\beta_e + \int_b^1 f_0\, d\beta_e \right), \tag{22}$$

where the integrand is

$$f_0 = \gamma\, e^{-\gamma/\Theta_e} \beta_e^{-4} \left(2\gamma^2\,\beta_e^5 + 6\beta_e + (3 - \beta_e^2) \ln\!\left(\frac{1-\beta_e}{1+\beta_e}\right) \right). \tag{23}$$

A Maclaurin expansion of the logarithm to order β_e^4 gives an adequate approximation

$$\int_0^b f_0\, d\beta_e \approx \int_0^b \gamma\, e^{-\gamma/\Theta_e} \beta_e \left(\gamma^2 + \frac{1}{3} - \frac{3}{5} + \left(\frac{1}{5} - \frac{3}{7}\right)\beta_e^2 + \left(\frac{1}{7} - \frac{1}{3}\right)\beta_e^4\right) d\beta_e \tag{24}$$

with no remaining divergent terms for the first integral in equation (22).

We derive $P_1^{MC}(s)$ from our Monte Carlo simulation by using the results of only the first (forced) scatterings. Figures 1a and 1b show our Monte Carlo results, P_1^{MC}, superimposed on P_1 from equations (19) and (20) for dimensionless temperatures $\Theta_e = 0.03$ and 0.3. The agreement is excellent, confirming that our Monte Carlo code is successfully reproducing $P_1(s)$.

2.3.2. Testing the Numerical Integral for the Intensity Change

We derive the intensity change from the FRDF using a numerical integral (equation [3]). The Kompaneets approximation leads to the following FRDF:

$$P_K = \frac{1}{\sqrt{4\pi y}} \exp\left(-\frac{(s-3y)^2}{4y}\right), \tag{25}$$

where the Compton y parameter is

$$y = \int n_e \sigma_T\, \Theta_e d\ell, \tag{26}$$

where n_e is the electron number density as a function of length in the line of sight measured by ℓ and Θ_e is the dimensionless temperature (for a discussion see for example Birkinshaw 1998; Molnar 1998). In order to check our numerical method, we used the Kompaneets FRDF (25) in the numerical integral in equation (3), and compared the resulting intensity change to that of obtained by the analytic solution for the Kompaneets approximation

$$\Delta I_K = y\, \frac{\imath_0 x^4 e^x}{(e^x-1)^2}\left(x\frac{e^x+1}{e^x-1} - 4\right), \tag{27}$$

where $\imath_0 = 2(k_B T_{CB})^3/(hc)^2)$. We concluded that our numerical method is accurate better than 0.1%.

2.3.3. Relativistic Corrections to Kompaneets equation

We also compare our results to those from the extended Kompaneets equation up to the 5th order in Θ_e (Itoh et al. 1998). Itoh et al. expressed the intensity change as

$$\Delta I = \frac{\Delta n}{n}\frac{\imath_0 x^3}{e^x - 1}, \tag{28}$$

and provided expressions for $\frac{\Delta n}{n}$ (note, that their y parameter is actually τ, the optical depth). On Figure 2 we plot $\Delta I/\tau$ from the Kompaneets approximation, from Itoh et al.'s expansion, and for our single scattering Monte Carlo results. From the figure we conclude that our single scattering Monte Carlo result agrees with that of Itoh et al. at low temperatures, $\Theta_e < 0.03$ ($T_e < 15$ keV). Deviations from the Itoh et al.'s result are already appearing at $\Theta_e = 0.03$, and become more pronounced at higher temperatures and high frequencies, as we would expect.

We conclude that our simulation method passes these two tests, and can now be used to calculate the effects of multiple scattering and bulk velocity on the SZ effect.

3. Results

We performed a number of simulations for uniform density spherical models which are either static or have radial infalls with constant gas velocity at all radii. These models cover a range of τ_0, the optical depth of zero impact parameter, electron temperature, T_e, and gas infall speed, β_r. Simulations with monochromatic incoming radiation were used to determine the FRDF.

In Figure 3 we show the FRDF for the static model with $\tau_0 = 0.05$ at seven different temperatures. At higher temperatures more photons scatter into higher energies, thus the FRDFs are broader, and have lower peaks (since they are normalized to unity). We show the effect of finite optical depth in Figure 4: higher optical depth leads to more scatterings, and therefore more photons scattered to higher energies. Even for an optical depth as large as $\tau_0 = 0.1$ the change in the function is relatively small. In Figure 5 we show the effect on the FRDF of gas infall. Larger infall velocities cause more up-scattering of the photons, and hence more spreading of the FRDF, but the most obvious change is that the sharp peak at $s = 0$ is smoothed out by the motion of the plasma. At lower temperatures bulk motion causes larger departures from the static FRDF since the infall speed is larger relative to the electron thermal velocity.

We used these results for the FRDF to calculate the spectra of scattered radiation by the convolution in equation (2). We derived the intensity change using equation (3). In the static model we have spherical symmetry and homogeneous and isotropic scattering conditions, therefore the same number of photons scatter out of as into the beam, and we can use the weight given in equation (4). In the case of infall we checked that equation (4) is still a good approximation in the regime in which we are interested.

We evaluated the emergent intensity change at zero impact parameter (i.e. through the center of the gas sphere), where $\tau = \tau_0$. In Figure 6 we show the intensity change ΔI for a static plasma for two optical depths and five temperatures. Non-zero optical depth causes only slight changes in the emerging radiation. Figure 7 shows the intensity change for a plasma with infall for two infall velocities and three plausible cluster temperatures. Only small changes in the spectrum are apparent, even with such large velocities.

One measure of the spectral deformation that has been used to quantify relative correction, and which is of use in determining the frequency at which to search for the KSZ effect, is the cross-over frequency. Challinor and Lasenby (1998a) and Birkinshaw (1998) suggested a linear expression for how the frequency changes with temperature, as

$$X_0^{lin} = 3.830(1 + 1.13\,\Theta_e), \tag{29}$$

while Itoh et al. 1998 suggested a quadratic approximation

$$X_0^{q} = 3.830(1 + 1.1674\,\Theta_e - 0.8533\,\Theta_e^2) \tag{30}$$

for most cluster temperatures. In Figure 8 we compare our Monte Carlo results with these and other expressions that include relativistic corrections. Our Monte Carlo results for single scattering are close to those obtained by numerical integration of the collision integral (Nozawa et al. 1998). Relativistic corrections of third and fifth order (Challinor and Lasenby 1998a; Nozawa et al. 1998), or the linear approximation (Challinor and Lasenby 1998a; Birkinshaw 1998) are of varying accuracy in describing the curve: the linear and third order expressions give the best results, but extending the series to the fifth order is much poorer. This is a consequence of the asymptotic nature of the series, as emphasized by Challinor and Lasenby (1998a).

Figures 9 and 10 show the cross-over frequency as a function of dimensionless temperature Θ_e for finite optical depth and infall velocity. Including a finite optical depth causes only a small change in the $X_0(\Theta_e)$ curve, and this change does not depend much on temperature. Based on our Monte Carlo simulations, we suggest the following approximation for the cross-over frequency for single scatterings in static spherical plasma for dimensionless temperature $\Theta_e \lesssim 0.3$:

$$X_0^{s}(\Theta_e) = 3.827\,(1 + 1.2038\,\Theta_e - 1.2567\,\Theta_e^2 + 0.9098\,\Theta_e^3), \tag{31}$$

which fits better than 0.01 % in this range with a shift from the optical depth dependence

$$\Delta X_0^{\tau}(\tau_0) = \tau_0(0.35 - 0.04416\,\Theta_e^{-0.5}), \tag{32}$$

which fits better than 0.005 % for $0.05 \leq \Theta_e \leq 0.3$, and about 0.1 % for lower temperatures, and $\tau_0 < 0.5$.

Figure (10) shows results for our spherical models with gas infall. As for non-zero optical depth, additional energy transfers occur because of motion of the gas. As we would expect, at low temperatures the contribution to the electron velocity from bulk motion is comparable to that from thermal motion, and an enhanced frequency shift results, while at high temperatures this contribution becomes negligible. Based on our Monte Carlo simulations, we suggest the following approximation for the cross-over frequency shift in plasma with infall for $0.01 \leq \Theta_e \leq 0.3$:

$$\Delta X_0^{\beta}(\Theta_e, \beta_r) = 0.224\,\beta_r^2\,\Theta_e^{-0.7}. \tag{33}$$

This formula fits the cross over frequency ν_0 better than about half a percent.

At small optical depth and bulk velocity we can assume that the shifts simply add, so that the final expression for the cross-over frequency becomes

$$X_0(\Theta_e, \tau_0, \beta_r) = X_0^s(\Theta_e) + \Delta X_0^{\tau}(\tau_0) + \Delta X_0^{\beta}(\Theta_e, \beta_r). \tag{34}$$

In Figure 11 we show the cross-over frequency as a function of temperature and optical depth in the parameter range ($\Theta_e \lesssim 0.04$, $\tau_0 \lesssim 0.05$) important for clusters of galaxies. From this figure we may come to the conclusion that, for clusters of galaxies, the optical depth effect on the cross-over frequency is more important than non-linear terms in the expansion in Θ_e. We provide more accurate fitting formulae for this range. From our models we find

$$X_0^{cl}(\Theta_e, \tau_0, \beta_r) = 3.829\,(1 + 1.1624\,\Theta_e - 0.68948\,\Theta_e^2) + 0.14\,\tau_0 + \Delta X_0^{\beta}(\Theta_e, \beta_r), \tag{35}$$

which fits better than 0.03 % for static models in this range of parameters. The optical depth independent first term is similar to the approximation provided by Itoh et al. (1998), which was obtained by numerically integrating the collision integral.

The relativistic corrections to the kinematic SZ effect (cluster radial bulk velocity, v_{rad}) have also been found to be important (Nozawa et al. 1998, Sazonov and Sunyaev 1998b) The shift was found to be

$$\Delta X_0^{kin}(\Theta_e, v_{rad}) = 300\,\frac{v_{rad}}{c}\left[\frac{a_1}{\Theta_e - \Theta_{min}} + \frac{a_2}{(\Theta_e - \Theta_{min})^2} + a_3 + a_4\,\Theta_e + a_5\,\Theta_e^2\right], \tag{36}$$

where v_{rad} is the radial velocity, $\Theta_{min} = 1.654 \times 10^{-3}$, $a_1 = 3.857 \times 10^{-3}$, $a_2 = -4.631 \times 10^{-6}$, $a_3 = 1.370 \times 10^{-2}$, $a_4 = 1.014 \times 10^{-2}$, and $a_5 = 0.01$ (Nozawa et al. 1998), which agrees well with Sazonov and Sunyaev's (1998b) result (expressed by a different fitting function). In Figure 11, long dashed lines represent the results of this kinematic effect of cluster radial velocity of $\pm$ 100 km s^{-1} ($X_0^{cl}(\Theta_e, 0) + \Delta X_0^{kin}(\Theta_e, v_{rad})$) Comparing our results for the shift in the cross-over frequency to results from relativistic kinematic effect, we conclude that a shift caused by an optical depth of 0.01 is equivalent to a shift caused by a radial velocity of about $v_{rad} = -10$ km s^{-1}.

We estimate the amplitudes of these effects on the hot cluster, Abell 2163, which was discussed by Holzapfel et al. (1997a). The maximum optical depth of the cluster is $\tau_0 = 0.01$, the temperature of the intracluster gas is close to $\Theta_e = 0.03$. Using our results for the static effect with the given temperature and maximum optical depth we get about 100 MHz shift to higher frequencies relative to the linear expression of Challinor and Lasenby (1998a). An infall velocity of $\beta_r = 0.01$ causes about an additional 15 MHz shift to higher frequencies relative to our result

for the static model. These shifts are small relative to the 20 GHz band width of the instrument of Holzapfel et al. (1997a) and the error in H_0 and cluster radial peculiar velocity from ignoring their presence would be about 10 % (if the SZ effect is measured at $x \gtrsim 5$) and 15 $\mathrm{km\,s^{-1}}$. By comparison, the component of primordial anisotropy in this scale corresponds to adding a velocity noise about ± 200 $\mathrm{km\,s^{-1}}$.

4. Conclusions

We investigated the effect of finite optical depth and bulk motion on inverse Compton scatterings in spherically symmetric uniform density mildly relativistic plasma. We assumed isotropic incoming radiation (CMBR), a relativistic Maxwellian distribution for the electron momenta, and scatterings in the Thomson limit. We demonstrated the usefulness of our Monte Carlo method for solving the radiative transfer problem, and calculated the static and kinematic SZ effects with different optical depth and gas infall velocities.

The solution of the extended Kompaneets equation (with corrections up to the fifth order) is equivalent to a single-scattering approximation, and significant deviations from it occur for hot clusters and at high frequencies. These deviations may be as large as 5 % of the intensity change and neglecting them could cause about a 10 % error in the Hubble constant. A finite optical depth causes further small changes in the SZ effect: these changes may exceed the relativistic correction terms. For typical cluster temperatures, an accurate expression for the cross-over frequency as a function of temperature, optical depth, and bulk motion is (35).

As it can seen from Figure 11, the cross-over frequency is sensitive to the cluster radial velocity, and less sensitive to the finite optical depth. Measurements of the cross-over frequency can, in principle, be used to determine the radial velocity of the cluster (e.g., as in Holzapfel et al. 1997b), with small extra corrections for optical depth and possible gas motion inside the cluster. However, the relatively strong variation of X_0 with Θ_e, compared to τ or β_r, suggests that the largest uncertainty will arise from the assumption of cluster isothermality, even if effects of confusion from primordial (and secondary) CMBR fluctuations can be excluded.

Finally we note that our method can be extended to any geometry, density distribution and complicated bulk motion as desired, and may be used to study the SZ effect in high temperature plasmas with or without bulk motion.

SMM is greatful for a full scholarship to Bristol University, where most of this work was done. This work was finished while SMM held a National Research Council-NASA/GSFC Research Associateship.

REFERENCES

Aghanim, N., Prunet, S., Forni, O., and Bouchet, F. R. , 1998, preprint, astro-ph/9803040, (A&A)

Birkinshaw, M., 1998, Physics Reports, in press

Birkinshaw, M and Gull, S. F. 1983, Nature, 302, 315

Challinor, A. and Lasenby, A., 1998. ApJ, 499, 1

Challinor, A. and Lasenby, A., 1998, preprint, astro-ph/9805329

Chandrasekhar, S. 1950, "Radiative Transfer", New York:Dover

Corman, E. G., 1970, Phys. Rev. D, 1, 2734

Fargion, D., Konoplich, R. V., and Salis, A. 1996, preprint, astro-ph/9606126

Fixsen, D.J., Cheng, E.S., Gales, J.M., Mather, J.C., Shafer, R.A., Wright, E.L., 1996. ApJ, 473, 576

Gull, S. F., and Garrett, A., 1998, in preparation

Gurvits, L. I. and Mitrofanov, I. G. 1983, 324, 349

Haardt, F., and Maraschi, L., 1993, ApJ, 413, 507

Holzapfel, W. L., Ade, P. A. R., Church, S. E., Mauskopf, P. D., Rephaeli, Y., Wilbanks, T. M., and Lange, A. E., 1997a, ApJ, 481, 35

Holzapfel et al. 1997b, ApJ, 480, 449

Hua, X., and Titarchuk, L., 1995, ApJ, 449, 188

Hughes, J. P., and Birkinshaw, M., 1998, ApJ, 501, 1

Itoh, N., Kohyama, Y., Nozawa, S., 1998, ApJ, 502, 7

Jones, F. C., 1968, Phys. Rev., 167, 1159

Kompaneets, A., S., 1957, Soviet Physics, JETP, 4, 730

Molnar, S.M., 1998, PhD Thesis, University of Bristol

Molnar, S. M., and Birkinshaw, M., 1998, in preparation

Nozawa, S., Itoh, N., Kohyama, Y., 1998, preprint, astro-ph/9804051

Pozdnyakov, L. A., Sobol I. M. and Sunyaev, R. A., 1983, Ap. and Space Phys. Rev. 2. 189.

Press, W. H., Teukolsky, S. A., Vetterling, W. T., and Flannery, B. P., 1992 "Numerical Recipes in C", Cambridge University Press, Cambridge

Psaltis, D, and Lamb, F. K., 1997, ApJ, 488, 881

Rees, M. J., and Sciama, D. W., 1968, Nature, 217, 511

Rephaeli, Y., 1995a, ApJ, 445, 33

Rephaeli, Y., 1995b, ARA&A, 33, 541

Rephaeli, Y. and Yankovich, D. 1997, ApJ, L55

Sazonov, S. Y., and Sunyaev, R. A., 1998a, Astronomy Letters, in press

Sazonov, S. Y., and Sunyaev, R. A., 1998b, reprint, astro-ph/9804125

Stebbins, A., 1997, preprint, astro-ph/9709065

Sunyaev, R. A., and Zel'dovich, Y. B., 1980, ARA&A, 18, 537

Wright, E. L., 1979, ApJ, 232, 348

This preprint was prepared with the AAS LaTeX macros v4.0.

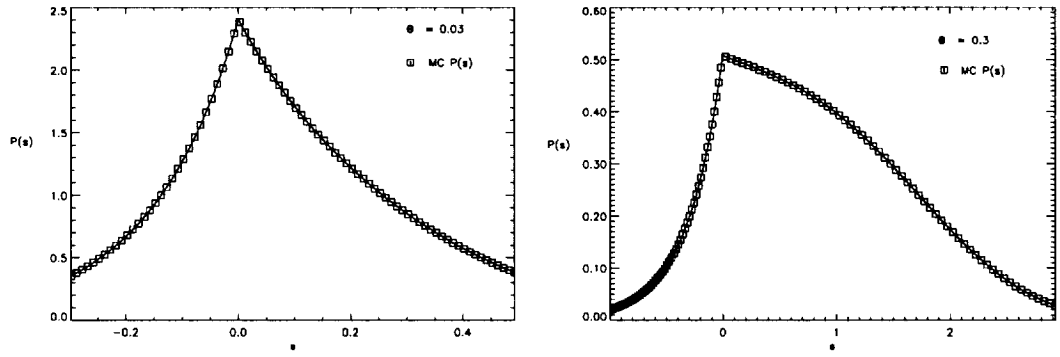

Fig. 1.— The frequency redistribution function, $P(s)$, for a static, single scattering case at dimensionless temperatures $\Theta_e = 0.03$ (a), or $\Theta_e = 0.3$ (b). The solid line shows the result from Rephaeli 1995b)'s semi-analytic method, the boxes with vertical error bars (too small to be visible) show results from our Monte Carlo simulations.

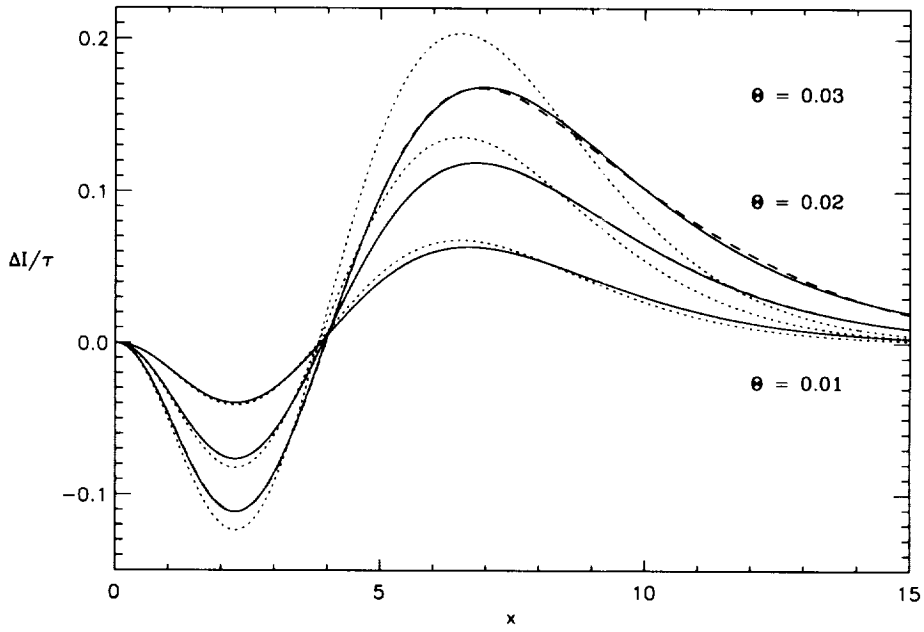

Fig. 2.— The intensity change $\Delta I/\tau$ (in units of $i_0 = 2(k_B T_{CB})^3/(hc)^2$) as a function of dimensionless frequency $x = h\nu/(k_B T_{CB})$ for dimensionless temperatures $\Theta_e = 0.01$, 0.02, and 0.03 in static spherically symmetric models. The solid, dashed and dotted lines are results from Monte Carlo method (single scattering), from relativistic corrections to the Kompaneets approximation (Itoh et al. 1997) and the Kompaneets approximation (Kompaneets 1957) respectively. Note that at low temperatures, $\Theta_e = 0.01$ and 0.02, the single scattering Monte Carlo method and the Kompaneets approximation with relativistic corrections give very similar results (the solid and dashed lines overlap).

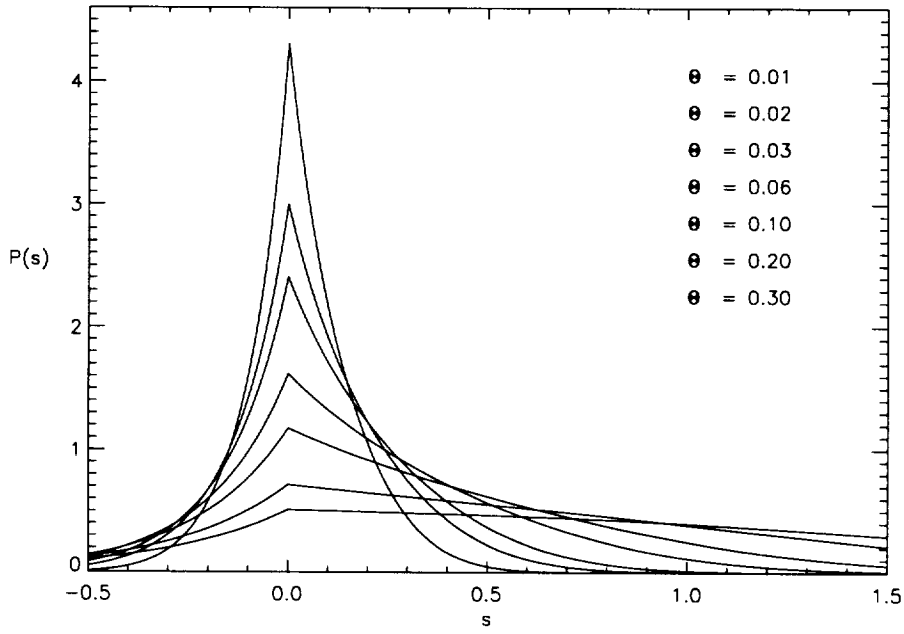

Fig. 3.— The frequency redistribution function, $P(s)$, from Monte Carlo simulation of static plasma with uniform density at seven temperatures. The higher the temperature, the lower the peak and wider the function due to larger energy transfers from the hot electrons to the photons.

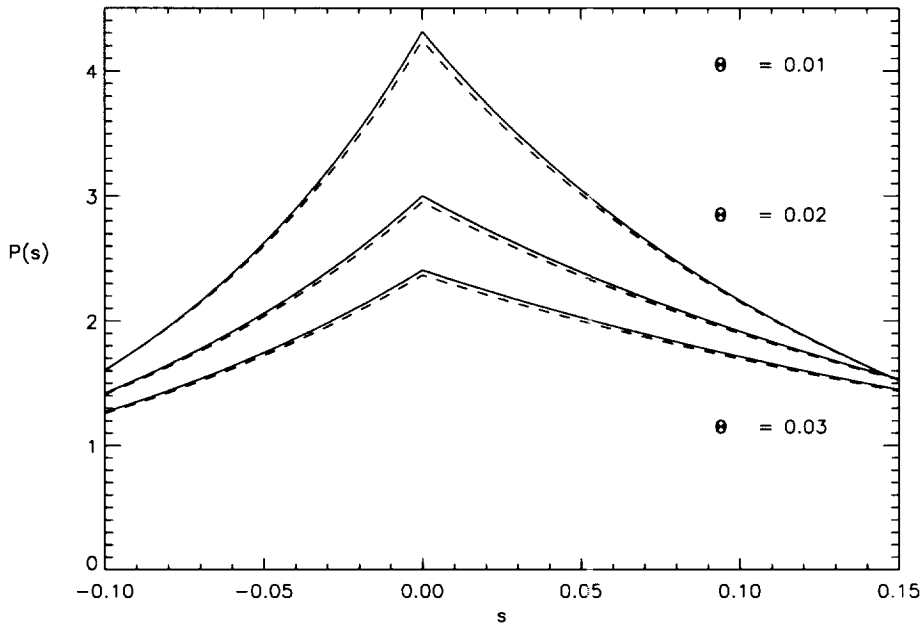

Fig. 4.— The inner part of the frequency redistribution function, $P(s)$, for static clusters with dimensionless temperatures $\Theta_e = 0.01$, 0.02, and 0.03. The solid and dashed lines show the extremes of single scattering and scattering with maximum optical depth $\tau_0 = 0.1$. More scatterings lead to more energetic photons, and hence more scattering from the line center to the high energy tail.

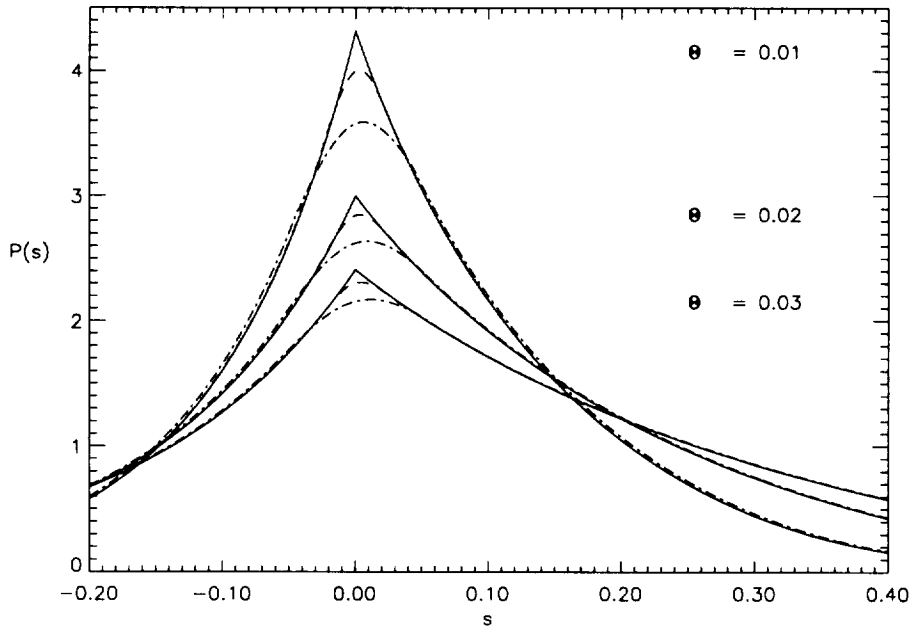

Fig. 5.— The single scattering frequency redistribution function, $P(s)$, for infalling plasma with dimensionless temperatures $\Theta_e = 0.01$, 0.02 and 0.03. The solid, dashed and dashed dot lines show results for models with infall velocities $\beta_r = 0$ (static), 0.03, and 0.05.

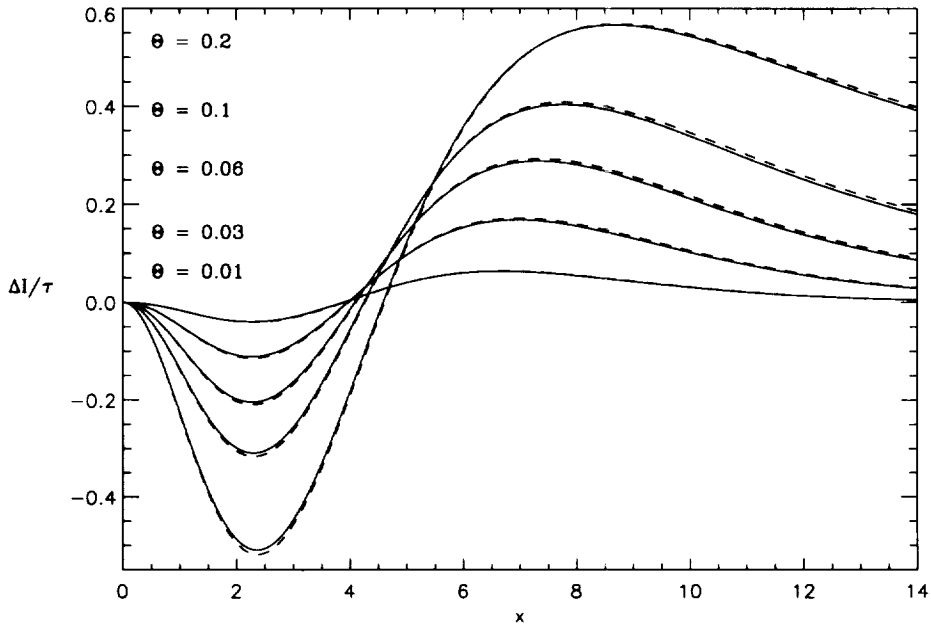

Fig. 6.— The intensity change $\Delta I/\tau$ (in units of $\imath_0 = 2(k_B T_{CB})^3/(hc)^2)$) as a function of dimensionless frequency $x = h\nu/(k_B T_{CB})$ for five dimensionless temperatures in static spherically symmetric models, for single scattering (solid lines) and $\tau_0 = 0.1$ (dashed lines).

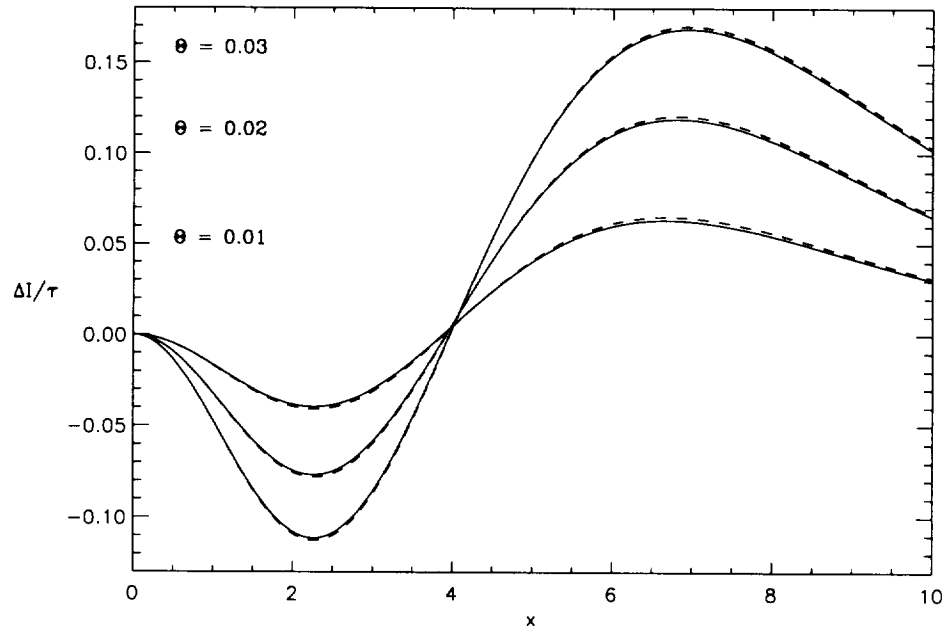

Fig. 7.— The intensity change $\Delta I/\tau$ (in units of $\imath_0 = 2(k_B T_{CB})^3/(hc)^2)$) as a function of dimensionless frequency $x = h\nu/(k_B T_{CB})$ for three dimensionless temperatures in spherically symmetric models with infall. Monte Carlo results are plotted using single scattering approximation for static gas (solid line) and gas with bulk motion ($\beta_r = 0.05$, dashed line).

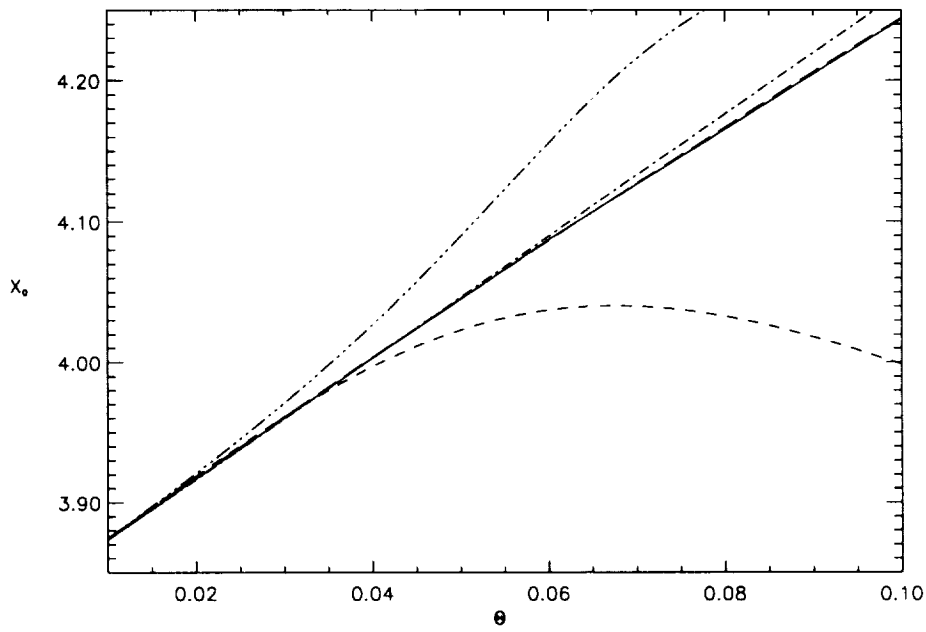

Fig. 8.— The cross-over frequency as a function of dimensionless temperature, Θ_e. The solid and long dashed lines show our Monte Carlo results for single scattering, and the results of a numerical evaluation of the collision integral (Nozawa et al 1998). The dashed dot line represents a linear approximation (Challinor and Lasenby 1998a; Birkinshaw 1998). The short dashed and dashed dot dot dot lines use relativistic corrections of third and fifth order in Θ_e.

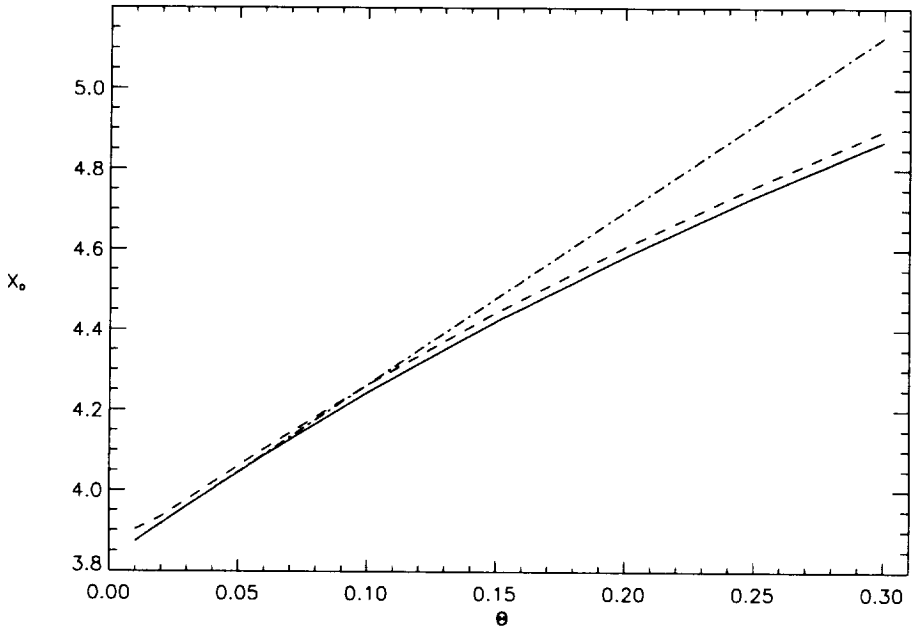

Fig. 9.— The cross-over frequency as a function of dimensionless temperature, Θ_e for static, spherically symmetric plasma. The solid and dashed lines are our results for single scattering and $\tau_0 = 0.1$, respectively. The dashed dot line shows a linear approximation (Challinor and Lasenby 1998a; Birkinshaw 1998). Finite optical depths cause a shift due to multiple scattering which is almost independent of the temperature.

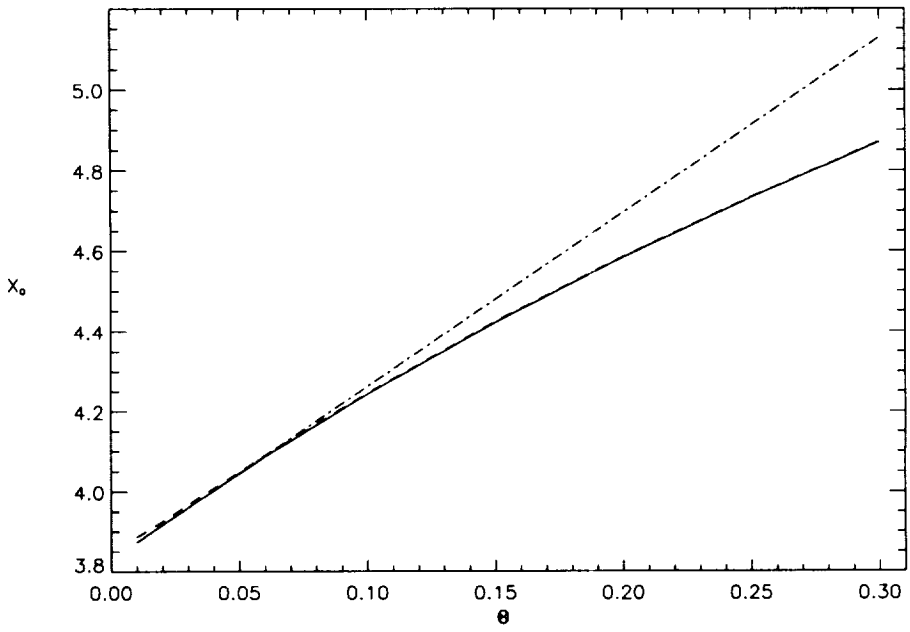

Fig. 10.— The cross-over frequency as a function of dimensionless temperature, Θ_e, for our spherically symmetric model with infall. The solid and dashed lines are for infall velocities $\beta_r = 0$ (reference static model) and $\beta_r = 0.05$. We used single scattering results to show only bulk motion effects. The dashed dot line shows a linear approximation (Challinor and Lasenby 1998a; Birkinshaw 1998). The effect of infall becomes inconsequential at high temperature since the infall speed becomes negligible relative to the thermal speed of the electron.

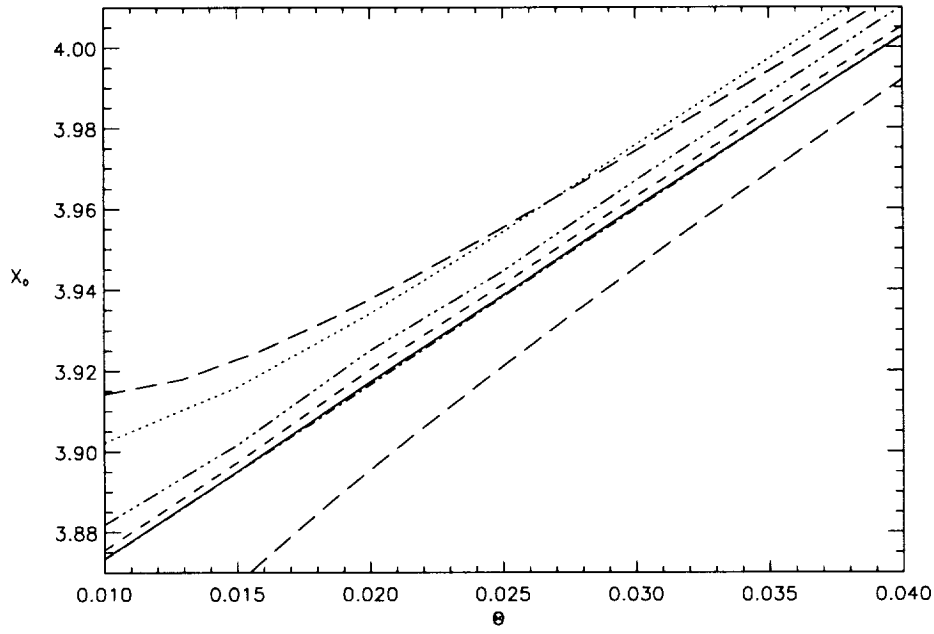

Fig. 11.— The cross-over frequency as a function of dimensionless temperature, Θ_e, for several optical depths in a static spherical plasma. Our Monte Carlo results are from single scattering (solid line), $\tau_0 = 0.02$ (short dashed line), 0.05 (dash, dot, dot, dot line), and 0.1 (dotted line). The dash-dot line, which is hardly distinguishable from the solid line, is the linear approximation of Challinor and Lasenby (1998a), and Birkinshaw (1998). As a comparison, we plot the (large) effect of a radial cluster velocity of $\pm$ 100 km s^{-1} (kinematic effect) with long dashed lines (Nozawa et al. 1998; Sazonov and Sunyaev 1998b).